



## Measuring shape variations of ECG waves through Time-Frequency Representations

Barbara Oficjalska, Hervé Rix, Emmanuel Chevalier, Jocelyne Fayn, André  
Varenne

### ► To cite this version:

Barbara Oficjalska, Hervé Rix, Emmanuel Chevalier, Jocelyne Fayn, André Varenne. Measuring shape variations of ECG waves through Time-Frequency Representations. European Signal Processing Conference EUSIPCO'94, Sep 1994, Edinburgh, United Kingdom. 1, pp.70-73, 1994. <hal-00545986>

**HAL Id: hal-00545986**

**<https://hal.archives-ouvertes.fr/hal-00545986>**

Submitted on 13 Dec 2010

**HAL** is a multi-disciplinary open access archive for the deposit and dissemination of scientific research documents, whether they are published or not. The documents may come from teaching and research institutions in France or abroad, or from public or private research centers.

L'archive ouverte pluridisciplinaire **HAL**, est destinée au dépôt et à la diffusion de documents scientifiques de niveau recherche, publiés ou non, émanant des établissements d'enseignement et de recherche français ou étrangers, des laboratoires publics ou privés.

## Measuring shape variations of ECG waves through Time-Frequency Representations

Barbara OFICJALSKA, Hervé RIX, Emmanuel CHEVALIER, Jocelyne FAYN†, André VARENNE††

13S CNRS - Université de Nice-Sophia Antipolis, Nice, France, Tel/Fax: +33 92942766 / 92942898,  
E-mail: oficjals@mimosas.unice.fr

† INSERM U121, Hôpital Cardiologique, Lyon, France

†† Laboratoire de Cardiologie (CRECEC), Hôpital Pasteur, Nice, France

**Abstract.** The Distribution Function Method in two dimensions (DFM-2D) is briefly presented as an extension of the previous Distribution Function Method in one dimension (DFM-1D). This novel method is applied to the estimation of shape difference between ECG waves through Time-Frequency Representations (Spectrograms). Shape variations due to drug action are followed along a day: for T-waves with Quinidine, for P-waves and QRS complexes with Cibenzoline. Clustering in two and three classes according to the "shape distance" is made too. The two methods, DFM-2D and DFM-1D, are compared using "pure shape distance", i.e. independently of scale changes, and a distance including width variations of the waves. The results concerning shape variations are coherent for the two methods, but in any case they are enhanced by using DFM-2D. In conclusion it appears that this novel method of shape difference measuring will be interesting in early detection and fine measurements of electrophysiological effects of cardiac drugs.

### 1. Introduction

Studying ECG signal variations involves the measure of interval lengths, cardiac wave durations and also shape variations of these waves, independently of shifts or scale changes. Little shape variations are difficult to detect by visual inspection and more difficult to measure specially in presence of noise. This is probably why this topic has been neglected till now. Nevertheless, some works in the domain can be cited [1-3]. Particularly in [2], the method used is the "Distribution Function Method" (DFM) [3]. This method gives the distance between the shapes of two 1D positive signals; included in the k-means algorithm it gives classes of equal shape signals, leading for example to the improvement of signal averaging [2]. In the present paper, we announce the extension of DFM to the two dimension case (DFM-2D); then we apply it to shape variations of Time-Frequency Representation (TFR) of ECG waves due to effects of drug absorption. The performances of DFM in one dimension (DFM-1D) and DFM-2D are compared.

### 2. The Distribution Function Method in two dimensions (DFM-2D)

Let  $f(x,y)$  and  $g(x,y)$  be two positive signals integrable on  $R^2$ . The equality of two shapes is defined by the existence of a relation of the form:

$$f(x,y) = kg\left(\frac{x-x_0}{\alpha}, \frac{y-y_0}{\beta}\right) \quad (1)$$

In the general case, for example when  $f$  and  $g$  represent the intensities of two images,  $\alpha$  and  $\beta$  are independent scale parameters. The shape identity notion can be restricted by linking  $\alpha$  and  $\beta$ , e.g. imposing  $\alpha = \beta$ .

Measuring shape differences makes use of the 2D normalized integrals:

$$F(x,y) = \int_{-\infty}^x \int_{-\infty}^y f(u,v)dvdu / \int_{-\infty}^{\infty} \int_{-\infty}^{\infty} f(u,v)dvdu \quad (2)$$

and a similar formula for  $G(x,y)$ . The sections at a fixed value of  $z$  give curves whose equations can be written as decreasing functions:

$$y = C_z(x) \text{ for } F \text{ and } y = D_z(x) \text{ for } G.$$

When signals  $f(x,y)$  and  $g(x,y)$  are the same shape,  $C_z$  and  $D_z$  are linked by:

$$C_z(x) = \beta D_z\left(\frac{x-x_0}{\alpha}\right) + y_0 \quad (3)$$

Position parameters  $x_0$  and  $y_0$  are eliminated by making the two mean points to coincide, i.e. assuming  $x_0=y_0=0$ . In the case where  $f$  and  $g$  are any two signals, measuring a shape difference needs the estimation of the scale parameter values  $\alpha^*$  and  $\beta^*$  which give the best fitting between  $C_z^*$ , where

$$C_z^*(x) = \beta^* D_z\left(\frac{x}{\alpha^*}\right) \quad (4)$$

and  $C_z(x)$ , according to the least mean square criterion. Then, we compute the mean residual associated to each  $z$ . The "shape distance"  $\Gamma(\alpha^*, \beta^*)$  is obtained by averaging these residuals for a series of  $z$  values going from 0 to 1. In the same way as for the DFM-1D, measuring a shape variation in the case of noisy signals needs a statistical determination of a threshold depending on the signal to noise ratio. Beyond this threshold, a shape difference is significant.

A particularly interesting case is that of 1D signals which can be compared by DFM-2D using the modulus of any TFR. Then  $\alpha$  and  $\beta$  (scale parameters on time and frequency respectively) are linked by:  $\beta=1/\alpha$ . The TFR we used - the Spectrogram - contains a temporal window: then it is necessary to fit the window width to the signal one. This fitting is made by DFM-1D estimation of the ratio of the two signal widths, called  $\alpha^-$ .

The conclusions on the results are practically the same if  $\alpha^*$  which optimizes  $\Gamma$  is replaced by  $\alpha^-$ ; this leads to reduce the computation time.

The detailed theory of DFM-2D is going to be submitted to *Signal Processing*.

### 3. Application to cardiac waves

Our study was performed on two young healthy adults who received only one dose of an antiarrhythmic drug. In case 1 it was 330mg of Quinidine (Ia class in Vaughan-Williams classification [4]), and in case 2 - 260mg of Cibenzoline (Ic class). ECG data were recorded using the three orthogonal leads X, Y, Z:

a) under the drug action (12 different records during 24 hours),  
b) under placebo (6 records at some of the hours from drug protocol, but a different day).

Two different systems of signal recording were used. In case 1 the sampling frequency was 500Hz with a 12bit resolution ( $\pm 10mV$  input). We studied the individual unfiltered T-waves, chosen as the most representative in 8 second records.

In case 2 the sampling frequency was 1kHz with a 16bit resolution ( $\pm 2.5mV$  input). We studied averaged QRS complexes and P-waves: in a 4 min. record the average was made over 50 beats aligned using the double level threshold on R-wave and chosen to have little R-R interval variations.

The studied signals are the root mean square of the 3 orthogonal leads X, Y, Z.

The results are composed of:

- the shape "distances" computed either by DFM-1D, or by DFM-2D applied to the Spectrogram with a gaussian window,
  - the clustering in 2 or 3 classes using the k-means algorithm.
- Lastly, we must emphasize that shape equality has been defined in two different ways: either shape identity in the strict sense, i.e. independently of any time scale variation ( $\alpha$  is a parameter to estimate - we use  $\alpha^-$ ), or a definition including both shape identity and width equality of the two signals ( $\alpha$  is enforced to 1). The separation between two classes  $i$  and  $j$  is measured by  $s_{ij} = d / (r_i + r_j)$ , where  $d$  is the distance between the class centres, and  $r_i, r_j$  are the mean radii of the classes.

#### 3.1 T-waves classification under Quinidine effect

The set of data contains 12 T-waves under Quinidine protocol (Table 1), and 6 with placebo.

no.	1	2	3	4	5	6
hour	7h30'	8h	8h15'	8h45'	9h15'	9h45'
time	-15'	+15'	+30'	+1h	+1h30'	+2h
no.	7	8	9	10	11	12
hour	10h15'	10h45'	12h45'	15h45'	19h45'	7h45'
time	+2h30'	+3h	+5h	+8h	+12h	+24h

Table 1. Numbers of waves, corresponding hours, and time after drug absorption.

The curves in Figure 1 show the shape variations (pure or combined with widening), along a drug absorption protocol between successive T-waves and the first one (without drug). These curves must be compared to similar curves corresponding to placebo absorption. It is obvious that the contrast between "drug curves" and "placebo curves" is much

higher when DFM-2D is used. When  $\alpha$  is enforced to 1, the contrast is much higher too. This means that width variations are important.

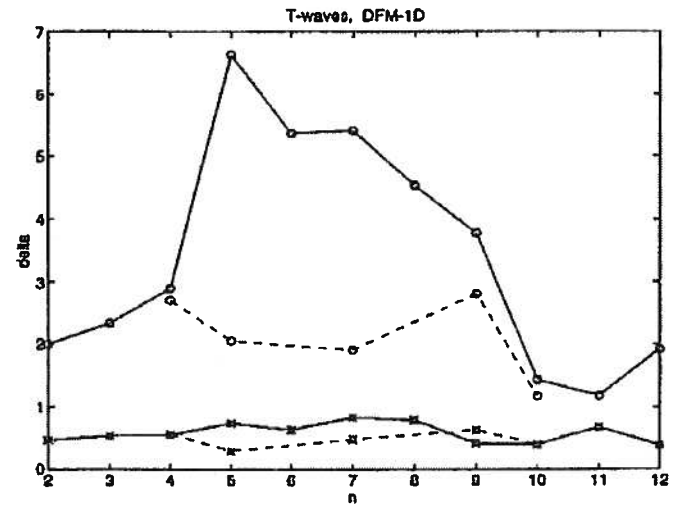


Figure 1.a.

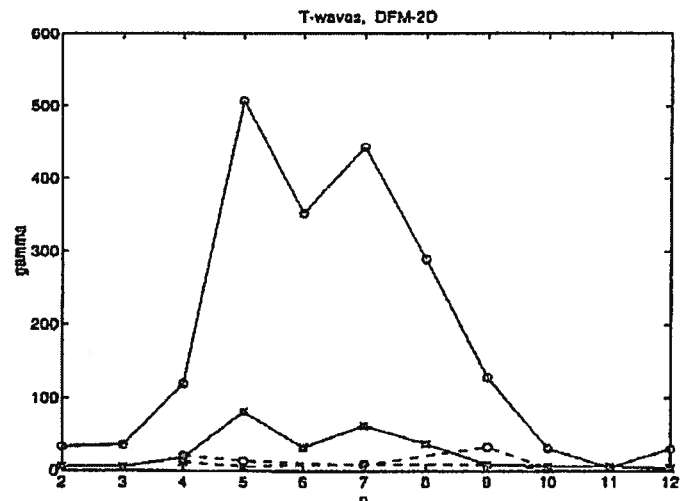


Figure 1.b.

Figure 1. Shape difference between T-wave no.  $n$  and T-wave no. 1 using: a) DFM-1D (delta), b) DFM-2D (gamma); o:  $\alpha=1$ , \*:  $\alpha=\alpha^-$ , solid line: Quinidine, dashed line: placebo.

The clustering (Table 2) in two classes is the same as well for the both methods (1D and 2D) as for the criterions of shape equality ( $\alpha=1$  and  $\alpha=\alpha^-$ ), with a value of parameter  $s_{ij}$  slightly better when  $\alpha$  is enforced to 1. On the other hand, the clustering in three classes is significant only when  $\alpha$  is enforced to 1. At last it is obvious that the separation measured by  $s_{ij}$  is higher with DFM-2D. The clustering process was repeated when the 6 waves from another day under the placebo were added to 12 waves under Quinidine protocol. The results are quasi-identical; the clustering is not due to the day or to the hour.

$\alpha$	$\alpha = 1$	$s_{ij}$	$\alpha = \alpha^-$	$s_{ij}$
1 D	{4 to 9}		{4 to 9}	
2 cl.	{1,2,3, 10,11,12}	$s_{12} = 2.7$	{1,2,3, 10,11,12}	$s_{12} = 1.1$
3 cl.	{5 to 8} {4,9,10} {1,2,3,11,12}	$s_{12} = 1.2$ $s_{13} = 4.3$ $s_{23} = 2.1$		
2 D	{4 to 9}		{4 to 9}	
2 cl.	{1,2,3, 10,11,12}	$s_{12} = 5.7$	{1,2,3, 10,11,12}	$s_{12} = 5.3$
3 cl.	{5 to 8} {4,9,10} {1,2,3,11,12}	$s_{12} = 4.0$ $s_{13} = 32.1$ $s_{23} = 7.7$		

Table 2. Clustering of the T-waves from the Quinidine protocol, in two classes (2 cl.) and three classes (3 cl.).

### 3.2 Averaged QRS complex and P-wave classification under Cibenzoline effect

The set of data contains: 12 QRS complexes and 12 P-waves under Cibenzoline protocol (Table 3); 6 QRS complexes and 6 P-waves with placebo.

no.	1	2	3	4	5	6
hour	8h35'	9h10'	9h40'	10h10'	10h40'	11h10'
time	-5'	+30'	+1h	+1h30'	+2h	+2h30'
no.	7	8	9	10	11	12
hour	11h40'	12h40'	14h40'	17h40'	22h40'	8h40'
time	+3h	+4h	+6h	+9h	+13h	+24h

Table 3. Numbers of waves, corresponding hours and time after drug absorption.

#### 3.2.1 QRS complex classification

Figure 2 is similar to Figure 1, but for QRS complexes. The contrast between "drug curves" and "placebo curves" is slightly higher when DFM-2D is used and when  $\alpha=1$ , but the differences are less important than for T-waves.

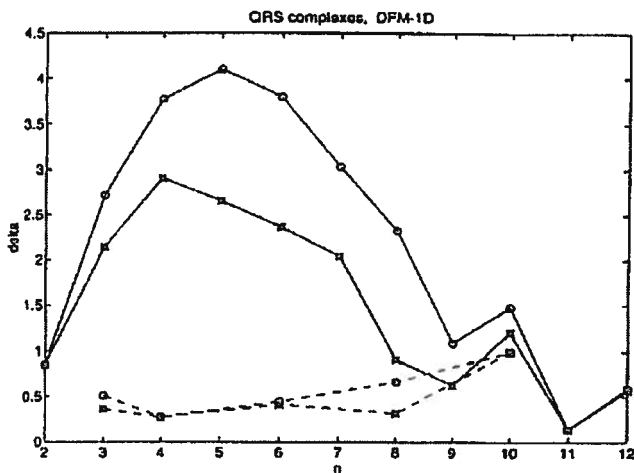


Figure 2.a.

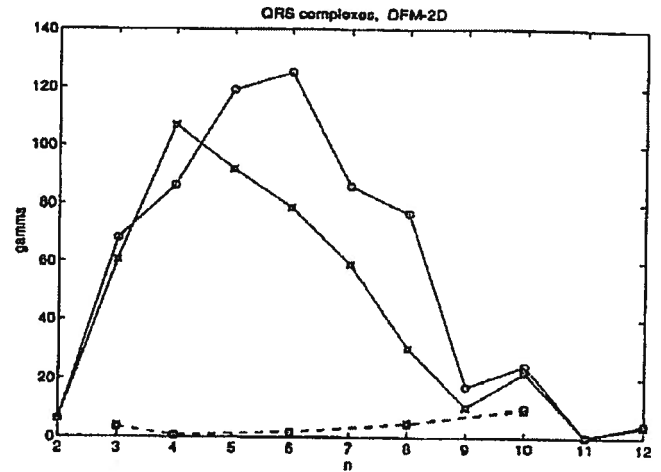


Figure 2.b.

Figure 2. Shape difference between QRS no. n and QRS no. 1 using: a) DFM-1D ( $\delta$ ), b) DFM-2D ( $\gamma$ );  $\alpha=1$ ,  $\alpha^-$ :  $\alpha=\alpha^-$ , solid line: Quinidine, dashed line: placebo.

The clustering (Table 4) in two classes is the same (except one complex) as well for the both methods (1D and 2D) as for the criterions of shape equality ( $\alpha=1$  and  $\alpha=\alpha^-$ ), with a value of parameter  $s_{ij}$  slightly better when  $\alpha$  is enforced to 1. On the other hand, the clustering in three classes is significant only when  $\alpha=\alpha^-$ . At last the separation measured by  $s_{ij}$  is higher with DFM-2D. The results obtained with addition of "placebo waves" are quasi-identical; the clustering is not due to the day or to the hour.

$\alpha$	$\alpha = 1$	$s_{ij}$	$\alpha = \alpha^-$	$s_{ij}$
1 D	{3 to 7}		{3 to 7}	
2 cl.	{1,2,8 to 12}	$s_{12} = 1.6$	{1,2,8 to 12}	$s_{12} = 1.5$
3 cl.			{3 to 7} {2,8,9,10,12} {1,11}	$s_{12} = 1.7$ $s_{13} = 3.1$ $s_{23} = 1.4$
2 D	{3 to 8}		{3 to 7}	
2 cl.	{1,2,9 to 12}	$s_{12} = 2.7$	{1,2,8 to 12}	$s_{12} = 2.0$
3 cl.			{3 to 7} {2,8,9,10,12} {1,11}	$s_{13} = 2.4$ $s_{13} = 6.2$ $s_{23} = 1.9$

Table 4. Clustering of the QRS complexes from the Cibenzoline protocol, in two classes (2 cl.) and three classes (3 cl.).

#### 3.2.2 P-wave classification

Figure 3 is similar to Figures 1 and 2, but for P-waves. The contrast between "drug curves" and "placebo curves" is slightly higher when DFM-2D is used and when  $\alpha=1$ . We can see a second peak for the wave no. 7 which appears only for  $\alpha=1$ , by the two methods. We have not find any clinical explanation of this phenomenon: further studies on several patients would be necessary.

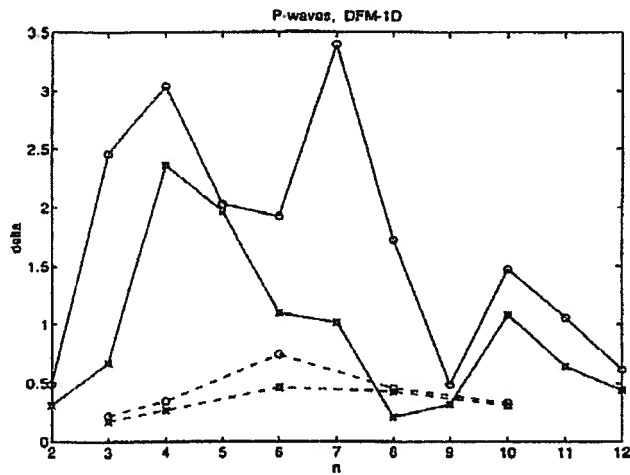


Figure 3.a.

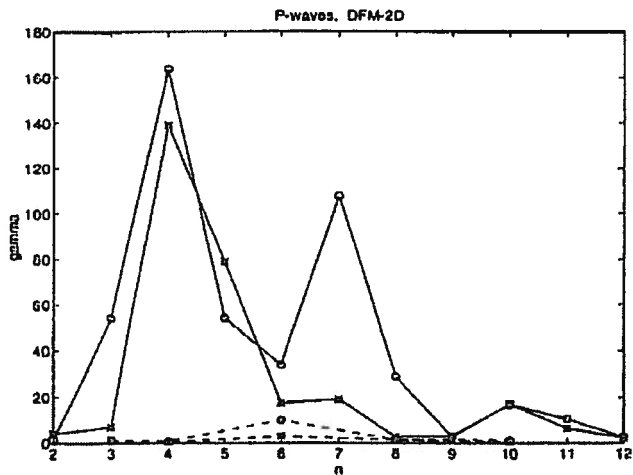


Figure 3.b.

Figure 3. Shape difference between P-wave no.  $n$  and P-wave no. 1 using: a) DFM-1D (delta), b) DFM-2D (gamma);  $\alpha=1$ , \*:  $\alpha=\alpha^*$ , solid line: Quinidine, dashed line: placebo.

$\alpha$	$\alpha = 1$	$s_{11}$	$\alpha = \alpha^*$	$s_{11}$
1D			{4,5}	
2 cl.			{1,2,3,6 to 12}	$s_{12}=1.7$
2D	{3,7,8}		{4,5}	
2 cl.	{1,2,4,5,6, 9 to 12}	$s_{12}=1.0$	{1,2,3,6 to 12}	$s_{12}=4.3$

Table 5. Clustering of the P-waves from the Cibenzoline protocol, in two classes (2 cl.) and three classes (3 cl.).

The clustering (Table 5) in two classes is the same for the both methods (1D and 2D) if  $\alpha=\alpha^*$ , with a value of parameter  $s_{ij}$  higher using DFM-2D. When  $\alpha$  is enforced to 1 we don't obtain a

significant clustering (DFM-1D) or a clustering which doesn't correspond to drug action (DFM-2D). No clustering in three classes is significant. At last the separation measured by  $s_{ij}$  is higher with DFM-2D. The results obtained with addition of "placebo waves" are quasi-identical, the clustering is not due to the day or to the hour.

#### 4. Conclusion

Different features can allow to follow the effects of drug absorption on ECG waves, for example the width of waves, their amplitude or their shape. In this paper we observe the variations of shape, either in the strict sense (independently of any time scale variation) or including width equality. We compared two methods based on Distribution Function: 1D, applied to the ECG waves in the time domain, or 2D applied to their Spectrograms.

Generally for "shape and width" distance both the variations and the class separation coefficients are higher than for "pure shape" distance. These variations and separation coefficients are also higher with DFM-2D than with DFM-1D. This is obvious specially for T-waves, which are signals whose frequencies are lower than P-wave and QRS complex ones, and whose widths present important variations under drug effect. But in some cases "pure shape" distance becomes more significant to interpret the curves and to cluster, specially for QRS complexes and P-waves. In any case the results concerning shape variations are enhanced by using DFM-2D compared to DFM-1D.

In conclusion it appears that this novel method of shape difference measuring will be interesting in early detection and fine measurements of electrophysiological effects of cardiac drugs.

#### References

- [1]. A.J. Bernal, D.E. Dick, M.W. Lutges (1975), Detection of digitalis toxicity by computerized electrocardiogram monitoring, *IEEE TBE*, vol. BME-22, no. 1.
- [2]. S. Jesus, H.Rix, A.Varenne (1986), Signal averaging using shape classification: application to high resolution ECG, *Proc. Int. Conf. EUSIPCO-86*, The Hague, The Netherlands, September 1986.
- [3]. H. Rix, J.P. Malenge (1980), Detecting small variations in shape, *IEEE Trans. Syst. Man and Cybern.* 10(2), 90-96.
- [4]. E.M. Vaughan-Williams (1992), Classifying Antiarrhythmic actions: by Facts or Speculation, *J. Clin. Pharmacol.* 32, 964-77.